Asia-Pacific Journal of Science and Technology: Volume: 27. Issue: 02. Article ID.: APST-27-02-15. Research Article

APST

Asia-Pacific Journal of Science and Technology

https://www.tci-thaijo.org/index.php/APST/index

Published by the Research and Graduate Studies,
Khon Kaen University, Thailand

Kinetic model of synthetic diesel production from stearic acid using MATLAB

Bantita Chomphutong[1], Penjit Srinophakun[1,*], Anusith Thanapimmetha[1], Maythee Saisriyoot[1] and Nutchapon Chiarasumran[1]

[1]Department of Chemical Engineering, Faculty of Engineering, Kasetsart University, Bangkok, Thailand
[*]Corresponding author: fengpjs@ku.ac.th

Received 22 September 2021
Revised 10 January 2021
Accepted 23 January 2021

Abstract

Hydrodeoxygenated vegetable oil is a second-generation alternative diesel. Oxygen in vegetable oil is removed through hydrodeoxygenation (HDO), decarbonylation (DCO), and decarboxylation (DCO_2) as the other main reactions in synthetic diesel production. The final products are hydrocarbon compounds with C15-C18 carbons, similar to traditional petroleum diesel. This study investigated the reaction mechanism and a kinetic model of synthetic diesel production from stearic acid (SA) with an $NiMo/Al_2O_3$ catalyst in the temperature range 270-300°C under excessive H_2. The kinetic model consisted of mass balance equations and rate law equations based on pseudo-first-order reactions. A MATLAB program was used for calculations. The results from the simulation demonstrated the %distribution of hydrocarbon products based on the proposed model was in good agreement with the experimental data. Furthermore, the results showed that the initial H_2 pressure greatly affected the composition of the hydrocarbon products and the reaction time. Therefore, the suggested conditions for synthetic diesel production from SA were an initial H_2 pressure of 75-80 bars, a reaction temperature of 300°C, an SA concentration of 5% wt, and a reaction time of 1.5 hours. These conditions produced an average low heating value of synthetic diesel of 44.22 Megajoule (MJ)/kg.

Keywords: Green diesel, Hydrodeoxygenation, Kinetic model, MATLAB, Stearic acid, Synthetic diesel

1. Introduction

Energy consumption is influenced by society and the economy. It is estimated that by 2040, global energy demand will increase by approximately 25% compared to current actual consumption [1]. Fossil fuels, including oil, coal, and natural gas, are the primary energy source that is now depleting rapidly as well as releasing large amounts of greenhouse gases (GHG) of which approximately 15% are released from transportation globally. Therefore, to reduce environmental problems, the development of alternative energy sources is necessary. According to the European Union's Biofuels 2020 Plan, 10% of the transportation section's fuels should be biofuels, and the target for this portion of biofuels will be even higher in the future [2].

Diesel fuel is classified as a general fuel with high combustion efficiency. Biodiesel, promoted as a standard replacement for traditional diesel fuel, is produced from vegetable oil and animal fat through transesterification [3]. However, the most impactful drawbacks of biodiesel are storage and compatibility with engines [4]. Therefore, the second generation of diesel was researched to find hydrocarbon compounds (C15-C18), similar to traditional diesel fuel [5]. In addition, second-generation biofuel is characterized by higher reductions in GHG emissions than current biodiesel and is produced from biomass [6].

Synthetic diesel can be produced from many natural products, including palm oil, soybean oil, sunflower oil, and jatropha oil [7]. The current study explored hydrodeoxygenation (HDO), decarbonylation (DCO), and decarboxylation (DCO_2) and took into account by-products, such as water, carbon dioxide (CO_2), carbon monoxide (CO), propane (C_3H_8), ethane (C_2H_6), and oxygen organic compounds (esters, aldehydes, and ketones).

Since the reaction pathway for renewable diesel production is complex, the current research aimed to develop the reaction mechanism based on a proposed kinetic model of synthetic diesel production from stearic acid (SA).

The MATLAB program was used for the simulation. An empirical kinetic model was developed and validated using secondary data. Finally, the influence was investigated of the initial hydrogen gas pressure on synthetic diesel products.

2. Material and method

2.1 Proposed mechanism of synthetic diesel production

Most researchers have proposed a mechanism of HDO of SA for synthetic diesel production. However, under the high temperature and pressure conditions this involves, many chemical reactions could occur. Therefore, the current study proposed a possible mechanism of HDO of SA, as shown in Figure 1.

2.2 Chemical reactions and rate law equations

As shown in Figure 1, SA can be converted directly to $C_{17}H_{36}$ and $C_{18}H_{38}$ through three primary reactions: decarboxylation (DCO_2, reaction number 1), decarbonylation (DCO, reaction number 2), and HDO (reaction number 3). In addition, the carboxylic functional group (-COOH) of the SA structure can be reduced to alcohol (stearyl alcohol) through reaction number 4 or to an aldehyde (octadecanal) through reaction number 5. Both reaction numbers 4 and 5 are reduction reactions where electrons from H_2 form bonds with oxygen molecules, resulting in water (H_2O).

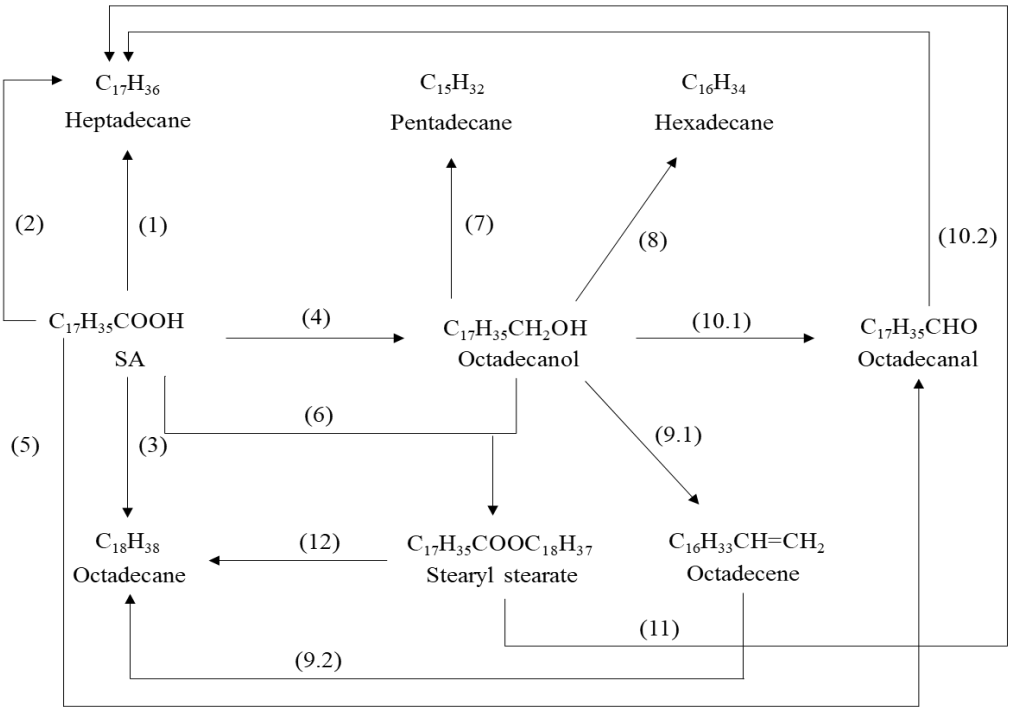

Figure 1 Proposed mechanism of synthetic diesel production from SA with NiMO catalysts at 270-300°C under excessive H_2.

Theoretically, stearyl alcohol can esterify with SA to form an ester, such as stearyl stearate ($C_{17}H_{35}COOC_{18}H_{37}$), through reaction number 6. Alternatively, stearyl alcohol can react with excess H_2 through HDO and release C_3H_8 (reaction number 7) or C_2H_6 (reaction number 8) to form $C_{15}H_{32}$ and $C_{16}H_{34}$, respectively. In addition, some stearyl alcohol is dehydrated (reaction number 9.1) due to heat released during HDO (reaction number 3, reaction number 7, reaction number 8, and reaction number 12) to form octadecene ($C_{16}H_{33}CH=CH_2$). According to various studies, the carbon-carbon bonds of unsaturated hydrocarbon compounds are rapidly converted to saturated hydrocarbons in atmospheric hydrogen through a hydrogenation reaction. Therefore, octadecene ($C_{16}H_{33}CH=CH_2$, reaction number 9.1) is promptly converted to octadecane ($C_{18}H_{38}$, reaction number 9.2). Consequently, chemical reaction number 9.1 is neglected. Stearyl alcohol can be oxidized to octadecanal (reaction number 10.1) and converted to heptadecane ($C_{17}H_{36}$). However, several experiments indicated the formation of only traces of octadecanal (reaction number 10.1) [8-10]. Aldehyde (octadecanal) has fewer stable molecules than alkane (reaction number 10.2); consequently, reaction number 10.1 is neglected.

Table 1 Reaction, chemical equations, and rate law equations of synthetic diesel products from HDO of SA proposed in this study.

Reaction No. (Refer to Figure 1)	Reaction	Chemical equation	Rate law equation
1	Decarboxylation (DCO_2)	$C_{17}H_{35}COOH \rightarrow C_{17}H_{36} + CO_2$	$r_1 = k_1 C_{C_{17}H_{35}COOH}$
2	Decarbonylation (DCO)	$C_{17}H_{35}COOH + H_2 \rightarrow C_{17}H_{36} + CO + H_2O$	$r_2 = k_2 C_{C_{17}H_{35}COOH} C_{0,H_2}$
3	Hydrodeoxygenation (HDO)	$C_{17}H_{35}COOH + 3H_2 \rightarrow C_{18}H_{38} + 2H_2O$	$r_3 = k_2 C_{C_{17}H_{35}COOH} C_{0,H_2}$
4	Reduction	$C_{17}H_{35}COOH + 2H_2 \rightarrow C_{17}H_{35}CH_2OH + H_2O$	$r_4 = k_4 C_{C_{17}H_{35}COOH} C_{0,H_2}$
5	Reduction and Decarbonylation (DCO)	$C_{17}H_{35}COOH + H_2 \rightarrow C_{17}H_{36}CO + H_2O$	$r_5 = k_5 C_{C_{17}H_{35}COOH} C_{0,H_2}$
6	Esterification	$C_{17}H_{35}COOH + C_{17}H_{35}CH_2OH \rightarrow C_{17}H_{35}COOC_{18}H_{37} + H_2O$	$r_6 = k_6 C_{C_{17}H_{35}COOH} C_{C_{17}H_{35}CH_2OH}$
7	Hydrodeoxygenation (HDO)	$C_{17}H_{35}CH_2OH + 2H_2 \rightarrow C_{15}H_{32} + C_3H_8 + H_2O$	$r_7 = k_7 C_{C_{17}H_{35}CH_2OH} C_{0,H_2}$
8	Hydrodeoxygenation (HDO)	$C_{17}H_{35}CH_2OH + 2H_2 \rightarrow C_{16}H_{34} + C_2H_6 + H_2O$	$r_8 = k_8 C_{C_{17}H_{35}CH_2OH} C_{0,H_2}$
9	Dehydration and Hydrogenation	$C_{17}H_{35}CH_2OH + H_2 \rightarrow C_{18}H_{38} + H_2O$	$r_9 = k_9 C_{C_{17}H_{35}CH_2OH} C_{0,H_2}$
10	Oxidation and Decarbonylation (DCO)	$C_{17}H_{35}CH_2OH \rightarrow C_{17}H_{36} + CO + H_2$	$r_{10} = k_{10} C_{C_{17}H_{35}CH_2OH}$
11	Decarbonylation (DCO)	$C_{17}H_{35}COOC_{18}H_{37} \rightarrow 2C_{17}H_{36} + 2CO$	$r_{11} = k_{11} C_{C_{17}H_{35}COOC_{18}H_{37}}$
12	Hydrodeoxygenation (HDO)	$C_{17}H_{35}COOC_{18}H_{37} + 4H_2 \rightarrow 2C_{18}H_{38} + 2H_2O$	$r_{12} = k_{12} C_{C_{17}H_{35}COOC_{18}H_{37}} C_{0,H_2}$

Table 2 Mass balance equations of synthetic diesel production from SA.

Liquid	Mass balance equation
SA	$\frac{dC_{C_{17}H_{35}COOH}}{dt} = -r_1 - r_2 - r_3 - r_4 - r_5 - r_6$
Pentadecane	$\frac{dC_{C_{15}H_{32}}}{dt} = r_7$
Hexadecane	$\frac{dC_{C_{16}H_{34}}}{dt} = r_8$
Heptadecane	$\frac{dC_{C_{17}H_{36}}}{dt} = r_1 + r_2 + r_5 + r_{10} + 2r_{11}$
Octadecane	$\frac{dC_{C_{18}H_{38}}}{dt} = r_3 + r_9 + 2r_{12}$
Stearyl alcohol	$\frac{dC_{C_{17}H_{35}CH_2OH}}{dt} = r_4 - r_6 - r_7 - r_8 - r_9 - r_{10}$
Stearyl stearate	$\frac{dC_{C_{17}H_{35}COOC_{18}H_{37}}}{dt} = r_6 - r_{11} - r_{12}$

Finally, stearyl stearate from reaction number 6 is hydrolyzed to $C_{17}H_{36}$ and $C_{18}H_{38}$ through DCO (reaction number 11) or HDO (reaction number 12) because of H_2O existing in the system. All proposed chemical reactions and equations are shown in Table 1. The rate law equations are pseudo-first-order reactions because of excess hydrogen feeding. The mass balance equations in the ordinary differential equation are proposed in Table 2. The MATLAB program was used to simulate all the kinetic model functions and to produce the %distribution of products in the liquid phase versus time.

2.3 Determining rate constants

All the rate constants in Table 1 were determined using least square method iterations (a standard regression analysis approach). First, the values of the initial rate constants (k_1-k_{12}) were obtained from various studies [8-12]. Next, these initial values were put into mass balance equations (Table 2). Then, the values of SA, heptadecane,

octadecane, and octadecanol were compared between the MATLAB and the experimental work [9,11]. Next, the recalculation was performed until the sum of squares residue was minimized. Then, the profiles of SA, heptadecane, octadecane, and octadecanol concentrations were plotted using the MATLAB simulator.

2.4 Model validation

The simulation was performed to obtain the profiles of the SA, heptadecane, octadecane, and octadecanol concentrations. Then, the simulation results were compared with the experimental data based on the coefficient of determination (R^2). Two sets of experimental data were used for the validation. Many researches have used one of two sets of conditions [8-12]. The first set of data was obtained from an experiment at a temperature of 220-280ºC and H_2 pressure of 20 bars on an $NiMo/Al_2O_3$ catalyst with the initial SA being 0.18 mol/L for a reaction time of 360 min [11]. The second set of data was obtained from an experiment at a temperature of 275-325ºC, H_2 pressure of 40-70 bars on a sulfide $NiMo/Al_2O_3$ catalyst at initial SA of 5% wt (0.0895 mol/L), and a reaction time of 180 min [9].

3. Results and discussion

3.1 Values of rate constants

Rate constants are essential and valuable parameters in a kinetic investigation. Table 3 shows the values of the rate constants obtained from the regression analysis. Two sets of experimental data were used. The first set was HDO of SA at 270ºC, H_2 pressure of 20 bars, SA concentration of 0.18 mol/L, and reaction time of 360 min. The second set was at a higher temperature of 300ºC and H_2 pressure of 50 bars, SA concentration of 5 wt% (0.0885 mol/L), and reaction time of 3 hours. If low temperature and pressure can be used, the operating cost will be lower, making synthetic diesel production feasible.

3.2 Validity

Figure 2 shows the SA, heptadecane, octadecane profiles, and octadecanol concentrations for both the experimental and calculated values. Based on the first set of data, the R^2 values for SA, heptadecane, and octadecane were 0.98, 0.92, and 1.00, respectively. At the end of the reaction (Figure 2A), the conversion rate of SA was 88.76%, and for intermediate (octadecanol) was 74.00%. On the other hand, Figure 2B shows the validity using the experimental results from the second set of data. The R^2 values of SA, heptadecane, and octadecane were 0.98, 0.96, and 0.96, respectively, and the conversion of SA was high at 98.60%. In comparison, intermediate (octadecanol) increased to a maximum of 28% and then decreased to less than 7% at the end of the experimental time. Thus, the simulation results fitted well with the experimental data. This good agreement confirmed the proposed reaction mechanism in Figure 1.

Table 3 Value of rate constants used in mass balance equations in Table 2

Rate constant	k_1	k_2	k_3	k_4	k_5	k_6	k_7	k_8	k_9	k_{10}	k_{11}	k_{12}
At 270°C	$1.95x10^{-6}$	$1.95 x10^{-6}$	$2.41 x10^{-6}$	$2.18 x10^{-4}$	$9.98 x10^{-7}$	$3.65 x10^{-6}$	$4.83 x10^{-7}$	$6.83 x10^{-7}$	$1.61 x10^{-5}$	$1.77 x10^{-6}$	$6.29 x10^{-6}$	$1.42 x10^{-6}$
At 300°C	$4.44 x10^{-5}$	$4.44 x10^{-5}$	$3.20 x10^{-5}$	$2.50 x10^{-4}$	$2.66 x10^{-6}$	$2.75 x10^{-5}$	$2.40 x10^{-7}$	$2.08 x10^{-7}$	$2.51 x10^{-4}$	$4.57 x10^{-5}$	$4.39 x10^{-5}$	$9.71 x10^{-4}$

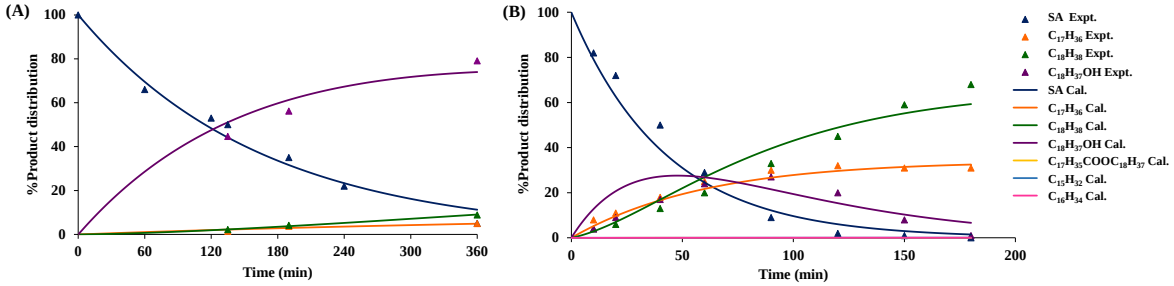

Figure 2 Concentration profiles of model predictions compared (A) first set of experimental data for 270°C reaction temperature, 20 bars H_2 pressure, 18 mol/L SA concentration, and 360 min reaction time; (B) second set of experimental data for 300°C reaction temperature, 50 bars H_2 pressure, 5%wt SA concentration, and 180 min reaction time. Triangular symbols are experimental values, and curves are model predictions.

3.3 Model simulation and prediction

Higher temperature and pressure (Figure 2B) produced higher amounts of octadecane (59.31%), heptadecane (32.46%), and SA conversion (98.60%). Therefore, the model was used for further investigation at a reaction temperature of 300°C and a broader range of H_2 pressures. Figure 3 shows the %SA distribution profiles when the H_2 pressure varied in the range 10-80 bars during 180 min of reaction time at a temperature of 300°C and an initial SA of 5%.

3.3.1 Effect of H_2 pressure on SA conversion

Figure 3 shows the profile of %SA distribution during 180 min of reaction time. Notably, when the H_2 pressure was higher, most of the SA reacted and was used up more rapidly, as shown in the %SA distribution in Figure 3. In addition, at an H_2 pressure of 50 bars, 1.48% SA remained unreacted (98.52% conversion) at 180 min. On the other hand, for the higher H_2 pressure at 80 bars, there was 99.84% SA conversion at 128 min of reaction time. For 95% SA conversion, the reaction times could be reduced to 128, 119, 109, 102, 95, 89, and 84 min at H_2 pressures of 50, 55, 60, 65, 70, 75, and 80 bars, respectively. Based on this simulation, the reaction time could be minimized.

3.3.2 Effect of H_2 pressure on SA, heptadecane, octadecane, and stearyl alcohol

The simulation was performed at a pressure over 50 bars to investigate the effect of H_2 on SA (reactant), heptadecane (product), octadecane (product), and stearyl alcohol (intermediate). As shown in Figure 4, octadecane was the main product with a %distribution of 60-70%. The octadecane distribution increased as the H_2 pressure increased. In contrast, the %heptadecane and stearyl alcohol decreased as the H_2 pressure increased. Therefore, the decrease in stearyl alcohol is preferable as it can change from an intermediate into final products.

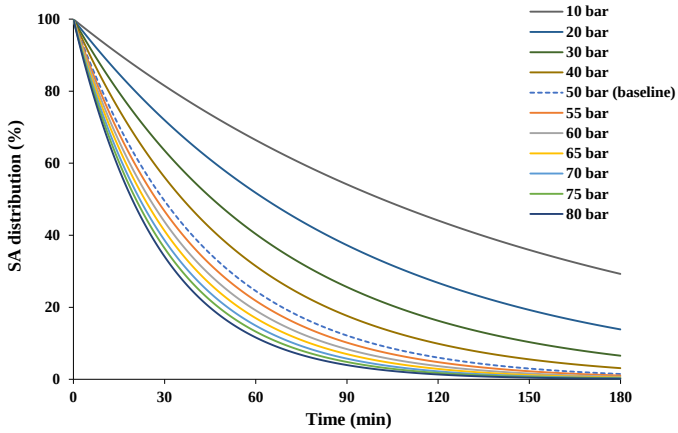

Figure 3 Influence of initial H_2 pressure (10-80 bars) on %SA distribution at 300°C reaction temperature, 5%wt SA concentration, and 180 min reaction time.

Furthermore, the simulation showed a greater level of octadecane than heptadecane at higher pressure. The simulation results confirmed the proposed mechanism in Figure 1. Stearyl alcohol was an intermediate product and was unstable, being further converted to 4 end-products, namely pentadecane (reaction number 7), hexadecane (reaction number 8), heptadecane (reaction numbers 10.1 and 10.2), and octadecane (reaction numbers 9.1 and 9.2). Both pentadecane and hexadecane were reported in trace amounts in other studies [9,11]. However, reaction number 9 became dominant; consequently, higher amounts of octadecane formed rather than heptadecane. Thus, the profile of stearyl alcohol gradually decreased as heptadecane slowly decreased to a constant level after 120 min of reaction time. In contrast, octadecane gradually increased toward the end of the reaction time. The higher pressure of 80 bars produced the highest final %octadecane distribution.

Figure 4C shows the profile of the main product, octadecane. It was possible that after 30 min of reaction time, octadecane was produced from reaction number 3. The level of heptadecane became steady at approximately 120 min. In contrast, octadecane kept increasing to approach its maximum level at the end of 180 min through reaction numbers 3 and 9. Hence, high pressure (high concentration of H_2) will promote these two reactions resulting in octadecane production. From this simulation, it can be concluded that a higher pressure is preferable for octadecane production. Notably, pentadecane (reaction number 7) and hexadecane (reaction number 8) were also produced but in trace amounts.

3.3.3 Prediction of low heating value

Finally, optimizing the operating cost was investigated based on the pressure, reaction time, and low heating value (LHV) of the synthetic diesel. Table 4 shows the reaction time at 95% SA conversion for different pressures from 50 to 80 bars, the %product distribution, and the fuel heating values. The estimation of LHV was based on the composition of synthetic diesel. The estimated LHV values for octadecane, heptadecane, hexadecane, and pentadecane were 44.21, 44.24, 44.27, and 44.30 Megajoule (MJ)/kg, respectively [4].

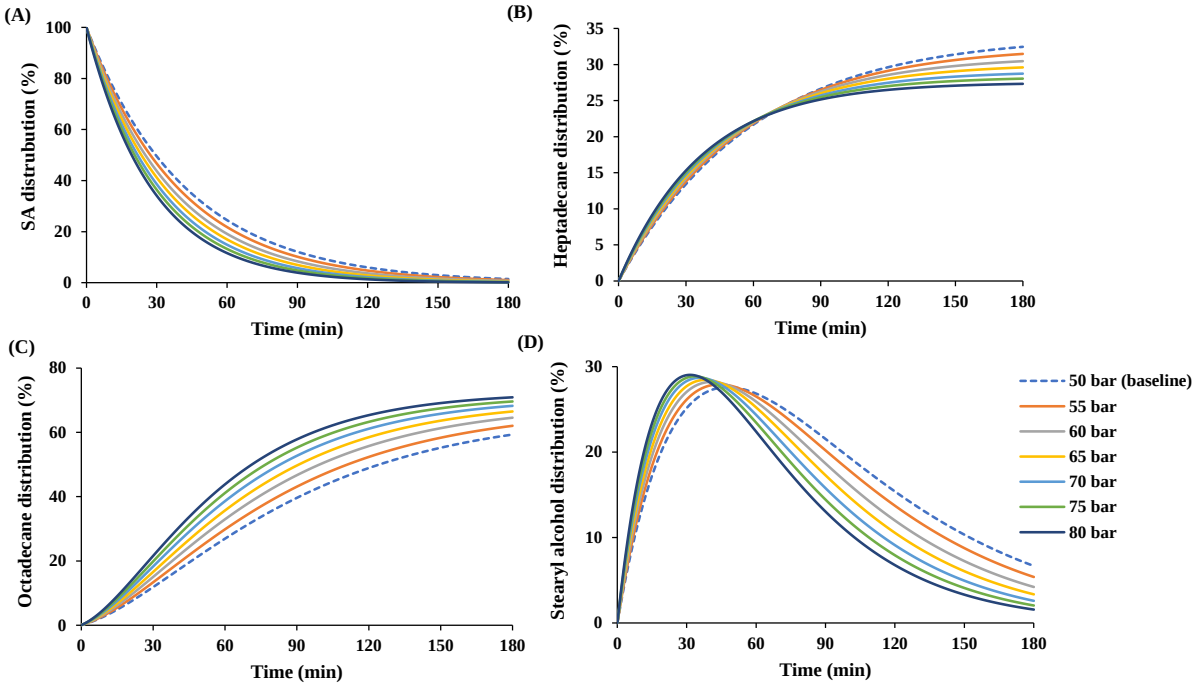

Figure 4 Influence of initial H_2 pressure (50-80 bars) on %product distribution at 300°C reaction temperature, 5%wt SA concentration, and 3 hours reaction time (A) SA (B) heptadecane (C) octadecane (D) stearyl alcohol.

Table 4 %Composition of synthetic diesel and LHV based on the second set of data for 300°C reaction temperature, 50-80 bars initial H_2 pressure, 5%wt SA concentration, and 3 hours reaction time.

H_2 Pressure (bars)	Reaction time at 95% SA conversion (min)	Final SA conversion (%)	%Composition of synthetic diesel				LHV (MJ/kg)
			$C_{17}H_{36}$	$C_{18}H_{38}$	$C_{15}H_{32}$	$C_{16}H_{34}$	
50	128	98.518	35.337	64.564	0.053	0.046	44.221
55	119	98.961	33.621	66.278	0.054	0.047	44.220
60	109	99.297	32.025	67.870	0.056	0.048	44.220
65	102	99.511	30.787	69.107	0.057	0.050	44.219
70	95	99.670	29.613	70.278	0.058	0.051	44.219
75	89	99.769	28.686	71.203	0.059	0.051	44.219
80	84	99.844	27.792	72.096	0.060	0.052	44.218

As shown in Table 4, when H_2 increased, the %conversion of SA was high, reaching 99% at 60 bars. Therefore, octadecane was the main product, with its production increasing with H_2 pressure. In comparison, the %heptadecane moved in the opposite direction. The expected amounts of pentadecane and hexadecane produced were low, as reported by other researchers [9,11]. Therefore, an H_2 pressure of 75-80 bars provided the highest octadecane composition. However, the LHV was relatively unchanged for any conditions of H_2 pressure in the range 50-80 bars. On the other hand, if 95% SA conversion is the target, then a higher H_2 pressure is recommended due to the reduced reaction time.

4. Conclusion

This research developed the reaction mechanism and proposed a kinetic model for synthetic diesel production from SA using a $NiMo/Al_2O_3$ catalyst for a reaction temperature range of 270-300°C under excessive H_2. The main reactions involved in the proposed mechanism were HDO, DCO, and DCO2, with other side reactions to form intermediate compounds, such as alcohols, aldehydes, esters, and alkenes. The rate constant (k) value was estimated at 270 and 300°C. The MATLAB program was used to simulate all the kinetic model functions. The

simulation results were evaluated by the predicted accuracy (based on R^2) of SA, heptadecane, and octadecane. The model simulation showed that the %distributions of hydrocarbon products were in agreement with both sets of experimental data. Furthermore, synthetic diesel production was investigated and simulated; the results showed that the initial H_2 pressure affected the hydrocarbon composition and reaction. Therefore, the suggested conditions for synthetic diesel production from SA were 75-80 bars initial H_2 pressure, 300°C reaction temperature, 5%wt SA concentration, and 1.5 hours reaction time. The average LHV of synthetic diesel under these conditions was 44.22 MJ/kg.

5. Acknowledgements

This work was supported by a scholarship from the Graduate School, Kasetsart University, Bangkok, Thailand and by the Faculty of Engineering, Kasetsart University who provided facilities. The Kasetsart University Research and Development (KURDI) provided editingsupport for the manuscript.

6. References

[1] Santamouris M. Energy Consumption and Environmental Quality of the Building Sector. Minimizing Energy Consumption, Energy Poverty and Global and Local Climate Change in the Built Environment: Innovating to Zero. Melbourne: Elsevier; 2019. p. 29-64.

[2] Uusitalo V, Väisänen S, Havukainen J, Havukainen M, Soukka R, Luoranen M. Carbon footprint of renewable diesel from palm oil, jatropha oil and rapeseed oil. Renew Energy. 2014;69:103-113.

[3] Snåre M, Kubičková I, Mäki-Arvela P, Eränen K, Murzin DY. Heterogeneous catalytic deoxygenation of stearic acid for production of biodiesel. Ind Eng Chem Res. 2006;45(16):5708-5715.

[4] Jeništová K, Hachemi I, Mäki-Arvela P, Kumar N, Peurla M, Čapek L, et al. Hydrodeoxygenation of stearic acid and tall oil fatty acids over Ni-alumina catalysts: influence of reaction parameters and kinetic modelling. Chem Eng J. 2017;316:401-409.

[5] Donnis B, Egeberg RG, Blom P, Knudsen KG. Hydroprocessing of bio-oils and oxygenates to hydrocarbons. Understanding the reaction routes. Top Catal. 2009;52(3):229-240.

[6] Kubička D, Kaluža L. Deoxygenation of vegetable oils over sulfided Ni, Mo and NiMo catalysts. Appl Catal A Gen. 2010;372(2):199-208.

[7] Boonrod B, Prapainainar C, Narataruksa P, Kantama A, Saibautrong W, Sudsakorn K, et al. Evaluating the environmental impacts of bio-hydrogenated diesel production from palm oil and fatty acid methyl ester through life cycle assessment. J Clean Prod. 2017;142:1210-1221.

[8] Arora P, Grennfelt EL, Olsson L, Creaser D. Kinetic study of hydrodeoxygenation of stearic acid as model compound for renewable oils. Chem Eng J. 2019;364:376-389.

[9] Arora P, Grennfelt EL, Olsson L, Creaser D. Kinetic study of hydrodeoxygenation of stearic acid as model compound for renewable oils. Chem Eng J. 2019;364:376-389.

[10] Kumar P, Yenumala SR, Maity SK, Shee D. Kinetics of hydrodeoxygenation of stearic acid using supported nickel catalysts: effects of supports. Appl Catal A Gen. 2014;471:28-38.

[11] Kumar P, Maity SK, Shee D. Role of NiMo alloy and Ni species in the performance of NiMo/alumina catalysts for hydrodeoxygenation of stearic acid: a kinetic study. ACS Omega. 2019;4(2):2833-2843.

[12] Kaluža L, Kubička D. The comparison of Co, Ni, Mo, CoMo and NiMo sulfided catalysts in rapeseed oil hydrodeoxygenation. React Kinet Mech Catal. 2017;122(1):333-341.